On Computational Neuroethology (and CybSPEED)

Manuel Graña

Computational Intelligence Group, UPV/EHU

This project has received funding from the European Union's Horizon 2020 research and innovation programme under the Marie Sklodowska-Curie grant agreement No 777720

Facultad de informatica, Universidad Complutense de Madrid

28/02/2019

Contents

- Introduction
- Brain activity: Neuroimage analysis
- Behavior –motion- analysis
- Combined neural and behavioral analysis
- The case study of CybSPEED
- Conclusions

Introduction

Computational ethology

- Ethology: study of animal behavior
  - phenomenological, causal, ontogenetic, and evolutionary aspects
  - its core is the description and characterization of behavior,
    - typically of intact freely moving animals in their natural environment.
    - Increasingly quantitative

- Computational support improves accurate observation
  - Interactive video annotation
  - Statistical and data processing
  - Machine Learning predictive models
- quantitative analysis of behavior allows to study correlation with neuronal activity
  - ➔ Neuroethology

Marker based Human motion capture

Facial active appearance models

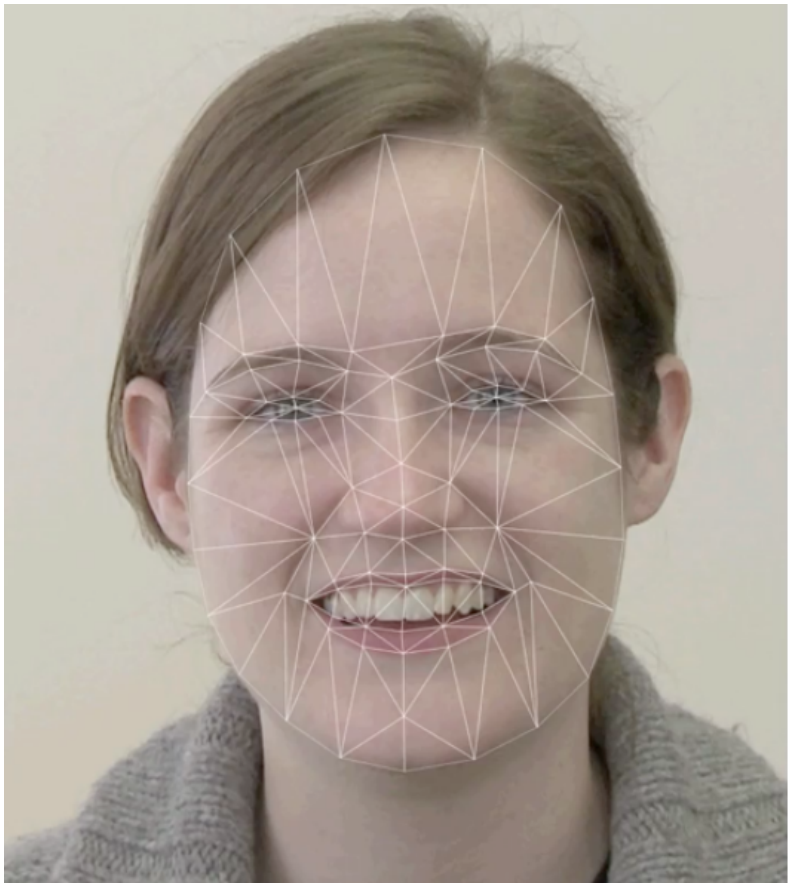

Neural activity and body motion

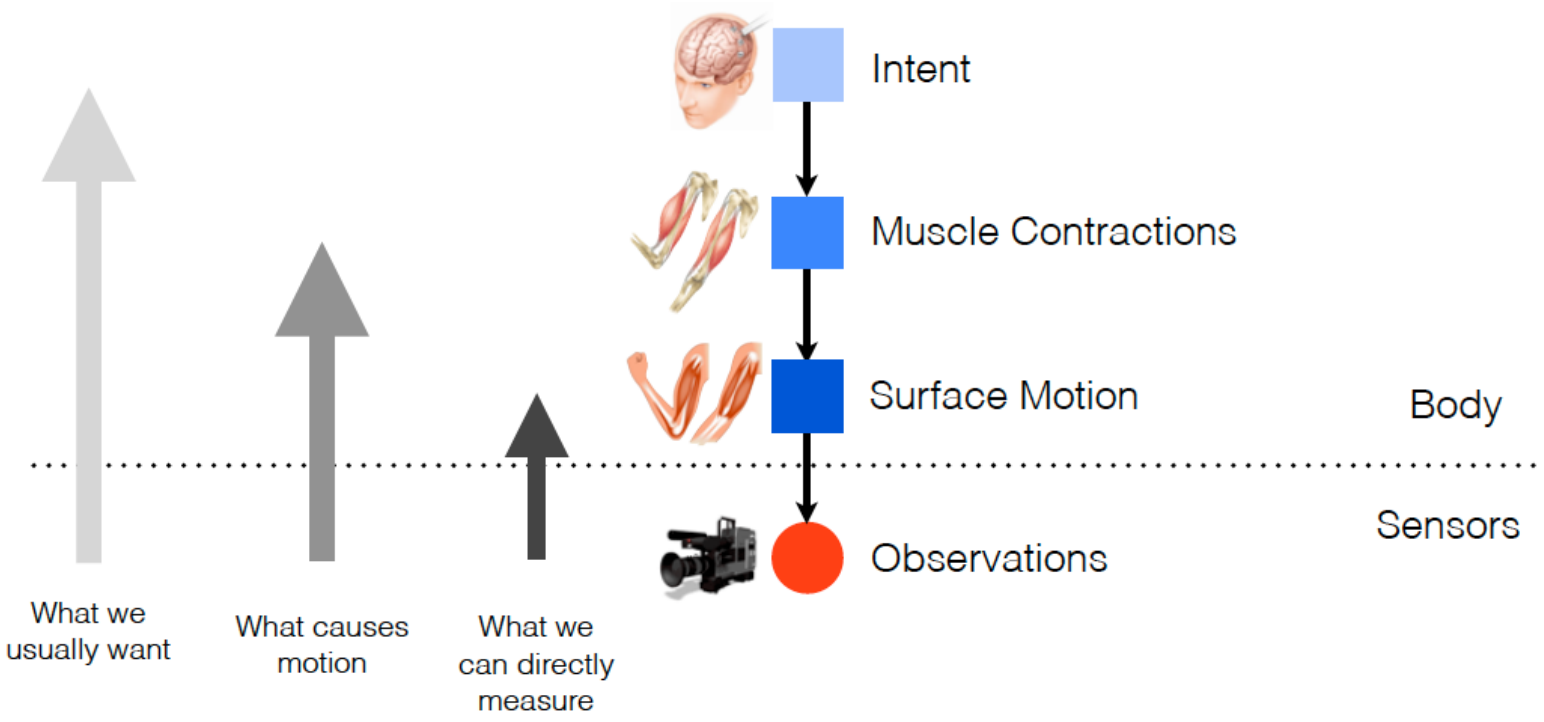

Motor Control

From Intent to Muscle Activation

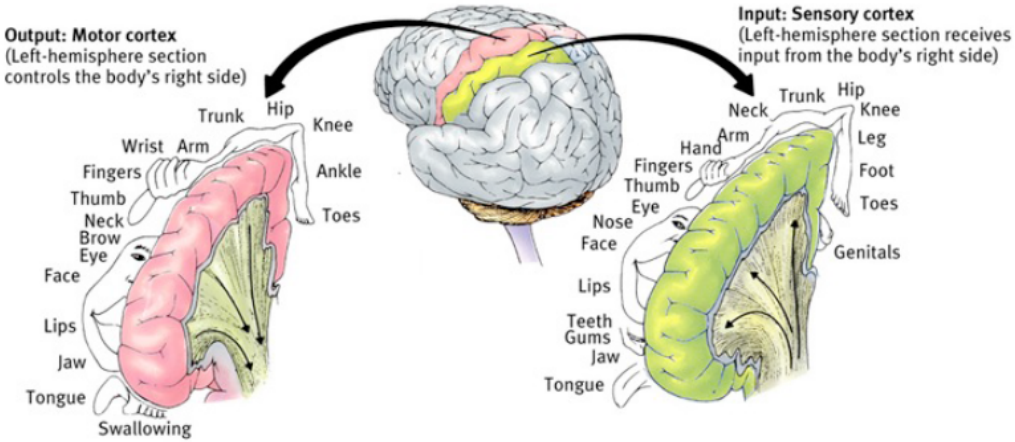

Ethology and Brain science

» Brain manifesto
» P 36 http://www.nih.gov/science/brain/2025/index.htm.

- **In summary,** the clever use of
  - virtual reality, machine learning, and miniaturized recording devices
- has the potential to dramatically increase our understanding of how neuronal activity underlies cognition and behavior.
- This path can be enabled by developing technologies to
  - quantify and interpret animal behavior,
    - at high temporal and spatial resolution,
  - reliably, objectively, over long periods of time,
  - under a broad set of conditions, and
  - in combination with concurrent measurement and manipulation of neuronal activity

Animal neuroethology

- New technologies for mapping, monitoring, and manipulating neural activity based on genetic targeting of specific neuron subtypes
  - beyond correlation to establish causal relationships between neural circuit activity and behavior.
  - critically dependent on the ability to assess quantitatively, and with a high degree of spatiotemporal precision, the behavioral consequences of neural circuit manipulations

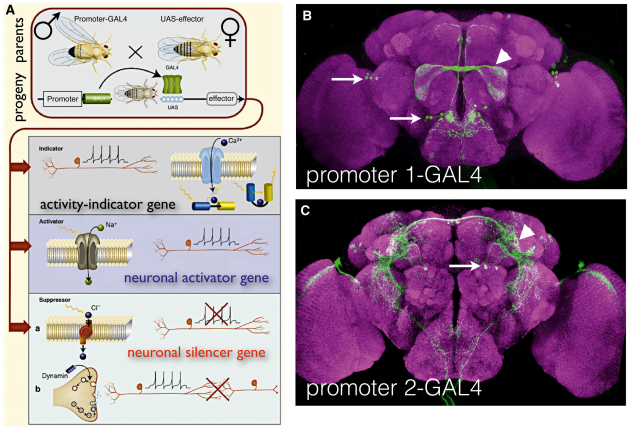

temperature-dependent manipulations of neuronal activity to identify a small cluster of neurons that controls aggression

Neuron 2014 84, 18-31DOI: (10.1016/j.neuron.2014.09.005

Applications human neuroethology

- Pharmacology: measuring the effect of treatments
- Improved diagnosis of neuro-behavioral conditions:
  - Autism Spectrum Condition
  - Neurodegenerative diseases
- Improved training techniques: sports
- Entertainment

Brain activity: Neuroimage analysis

Neuroimage analysis

- Objective: to find brain localizations related to psychologic/psychiatric conditions
  - Anatomical differences
  - Functional differences: brain networks
- Material: various modalities of MRI
  - T1, DWI, TWI, for anatomical and connectivity
  - fMRI, rs-fMRI for functional analysis
- Computational resources:
  - Signal processing: preprocessing, feature extraction
  - Massive statistical tests
  - Machine learning: supervised: SVM… deep learning

Chyzhyk D, Graña M, Öngür D, Shinn AK. Discrimination of Schizophrenia Auditory Hallucinators by Machine Learning of Resting-State Functional MRI.International Journal of Neural Systems 25(3):1550007, 2015

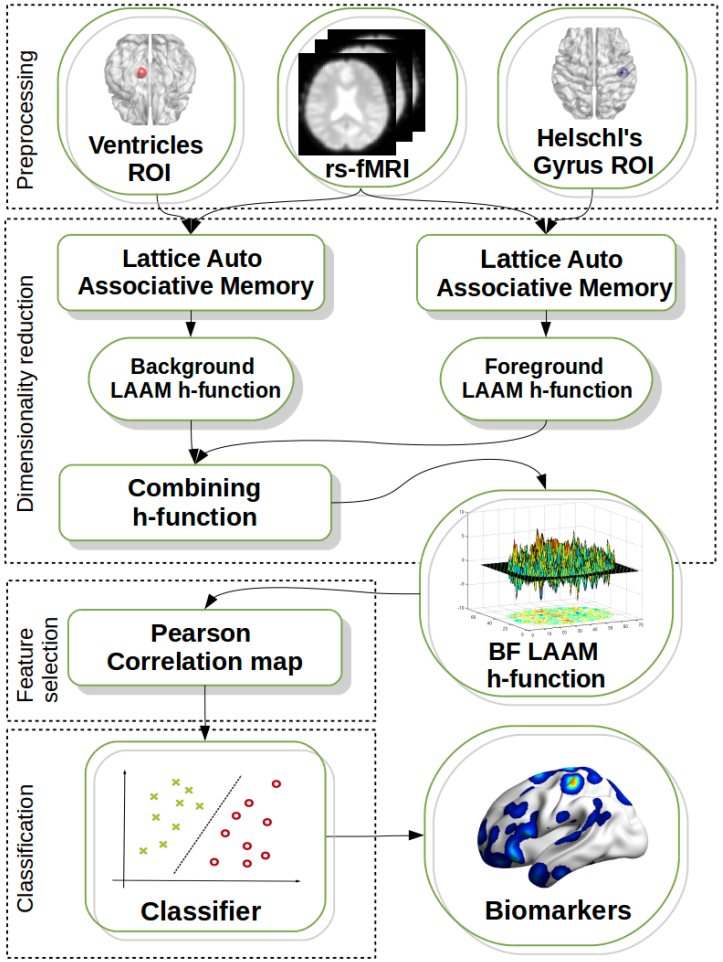

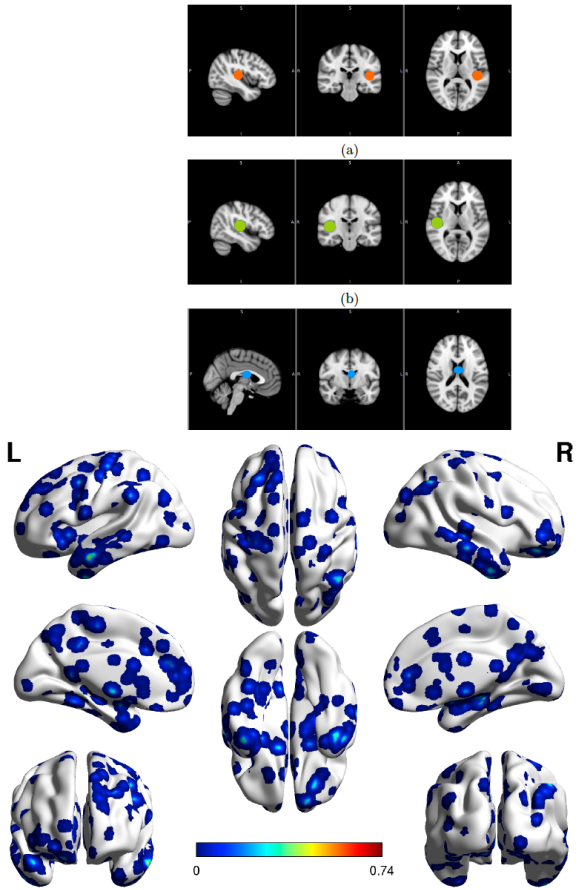

Fig. 3. Localization of feature voxel sites selected from the BF-LAAM *h*-function map with foreground seed extracted from the LHG ROI, when discriminating SZAH from SZnAH populations. Colorbar is proportional to voxel saliency .

Table 5. Cortical brain regions of the feature voxel sites corresponding to **ReHo** and **fALFF** feature vectors of size 1000, for the classification of **SZAH vs. SZNAH**. CS = Cluster size. H=Brain Hemisphere, L=Left, R=Right.

ReHo			Coordinates			fALFF			Coordinates		
Region	H	CS	x	y	z	Region	H	CS	x	y	z
Inferior Frontal Gyrus	L	25	-54	27	24	Frontal Medial Cortex	R	28	12	39	-15
Frontal Orbital Cortex	L	37	-48	24	-9	Frontal Pole	R	43	21	54	-15
Frontal Operculum Cortex	R	14	42	24	6	Middle Temporal Gyrus	L/R	17/7	-57/57	-39/-42	-12/-12
Superior Frontal Gyrus	L	13	-18	6	66	Central Opercular Cortex	L	14	-36	9	12
Superior Temporal Gyrus	L	18	-69	-6	0	Insular Cortex	R	14	27	18	0
Inferior Temporal Gyrus	R	13	42	0	-51	Cingulate Gyrus	L	7	-15	9	30
Temporal Pole	L/R	14/16	-45/39	9/6	-36/-39	Paracingulate Gyrus	L	14	-15	30	24
Precentral Gyrus	L/R	21	18	-18	72						
Parietal Operculum Cortex	R	13	51	-30	27						
Supramarginal Gyrus	R	13	30	-48	33						
Cingulate Gyrus, posterior division	R	20	9	-39	3						
Subcallosal Cortex	L	36	-3	30	0						
Precentral Gyrus	L	41	-30	-21	48						

	Measure	Feat.Map.	HG	500	1000	5000	10000
SZAH vs. SZNAH	FC	OS-LAAM	L	**97.5**	**97.5**	**97.5**	**92.5**
			R	**92.5**	**92.5**	**95**	**95.2**
		BF-LAAM	L	**100**	**97.5**	**95**	**90**
			R	**100**	**100**	**100**	**100**
	LA	ReHo	-	**100**	**100**	**100**	**100**
		ALFF	-	85	87.5	**92.5**	**92.5**
		fALFF	-	**97.5**	**100**	**100**	**97.5**
SZAH vs. HC	FC	OS-LAAM	L	43.7	42.7	30.7	28.3
			R	52.3	50	33	28
		BF-LAAM	L	**96.7**	**98**	**96.3**	**93**
			R	**98.3**	**96**	**92.7**	**93**
	LA	ReHo	-	**98**	**98.3**	**96.7**	**96.6**
		ALFF	-	48.7	49	30.3	31.7
		fALFF	-	**100**	**100**	**98.3**	**98.3**
SZnAH vs. HC	FC	OS-LAAM	L	65	63	59.5	55
			R	74	70	60	55
		BF-LAAM	L	**100**	**100**	**95.5**	**93**
			R	**100**	**98**	**95.5**	**93.5**
	LA	ReHo	-	**97.5**	**98**	**95.5**	**96**
		ALFF	-	78	76	62	53
		fALFF	-	**100**	**100**	**100**	**100**
SZ vs. HC	FC	OS-LAAM	L	32.4	31	26	25
			R	41.4	36.7	26.9	25.2
		BF-LAAM	L	**95.5**	**97.1**	88.6	85.7
			R	**94.3**	**91.2**	86.7	87.1
	LA	ReHo	-	**95.7**	**95.7**	**97**	**95.5**
		ALFF	-	48.8	42.9	35.2	35.2
		fALFF	-	**98.5**	**100**	**97.1**	**97.1**

	Measure	Feat.Map.	HG	500	1000	5000	10000
SZAH vs. SZNAH	FC	OS-LAAM	L	**100**	**100**	**100**	**100**
			R	**100**	**100**	**100**	**100**
		BF-LAAM	L	**100**	**100**	**100**	**100**
			R	**100**	**100**	**100**	**100**
	LA	ReHo	-	**100**	**100**	**100**	**100**
		ALFF	-	**96.7**	**96.7**	**100**	**100**
		fALFF	-	**100**	**100**	**100**	**100**
SZAH vs. HC	FC	OS-LAAM	L	28.3	21.7	11.7	8.3
			R	38.3	30	18.3	10
		BF-LAAM	L	**96.7**	**96.7**	**93.3**	85
			R	**96.7**	**93.3**	**91.7**	**93.3**
	LA	ReHo	-	**100**	**100**	**96.6**	**96.7**
		ALFF	-	45	41.7	21.7	18.3
		fALFF	-	**100**	**100**	**100**	**100**
SZNAH vs. HC	FC	OS-LAAM	L	40	40	20	15
			R	50	40	25	20
		BF-LAAM	L	**100**	**100**	**90**	80
			R	**100**	**95**	**90**	85
	LA	ReHo	-	**100**	**100**	**95**	**95**
		ALFF	-	60	50	30	20
		fALFF	-	**100**	**100**	**100**	**100**
SZ vs. HC	FC	OS-LAAM	L	30	27.5	17.5	20
			R	40	35	25	22.5
		BF-LAAM	L	**97.5**	**100**	**95**	**92.5**
			R	**95**	**95**	**90**	**92.5**
	LA	ReHo	-	**100**	**100**	**96.6**	**96.7**
		ALFF	-	47.5	45	37.5	35
		fALFF	-	**97.5**	**100**	**97.5**	**97.5**

Manuel Graña, Leire Ozaeta, Darya Chyzhyk

Dynamic Causal Modeling and Machine Learning for Effective Connectivity in Auditory Hallucination Neurocomputing Volumes 326–327, 31 January 2019, Pages 61-68

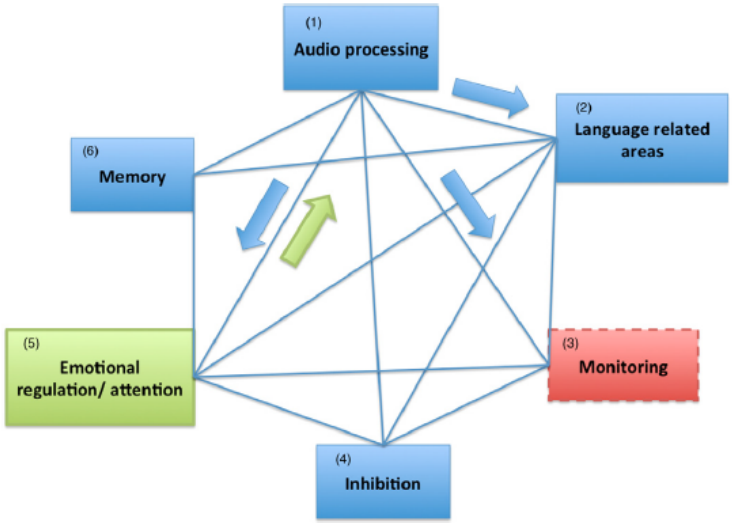

Fig. 1. Abstract functional model of the brain functional interactions while experiencing an auditory hallucination. The arrows indicate the general expected hallucinating signal path, starting in the auditory cortex and traveling to emotional regulation/attention, language related and monitoring areas. The areas with thicker border are more activated in the hallucination prone brain, while areas with discontinued border are less activated.

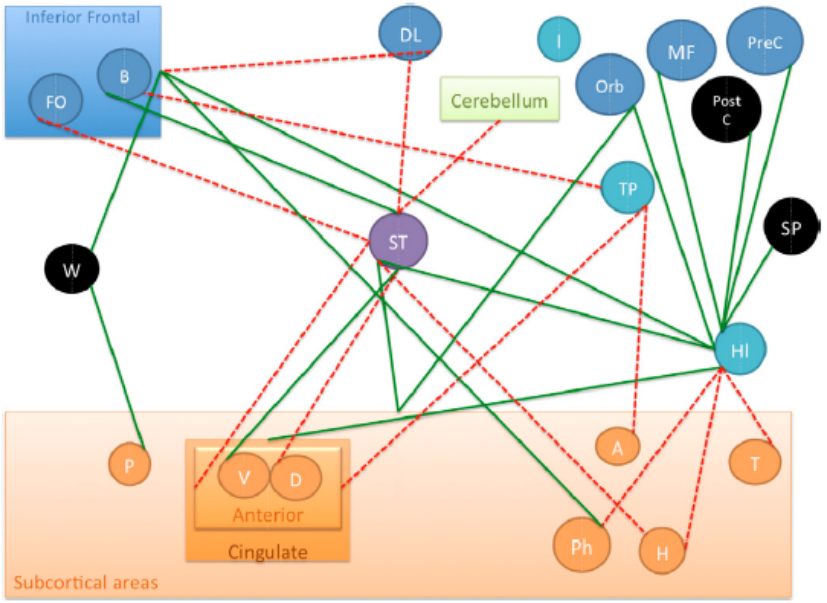

Fig. 2. A detailed anatomical model of interacting brain regions underlying the abstract functional model of auditive hallucinations. Identified areas are as follows: orbitofrontal gyrus (Obr), frontal dorsolateral gyrus (DL), middle frontal gyrus (MF), precentral gyrus (PreC), Broca's area (B), frontal operculum (FO), superior parietal (SP), Wernickles area (W), postcentral gyrus (PostC), amygdala (A), Thalamus (T), putamen (P), ventral anterior anterior cingulate (V), dorsal anterior cingulate (D), hippocampus (H), parahippocamus (Ph), insula (I), Heschl's gyrus (Hl), Temporoparietal gyrus (TP), superior temporal (ST).

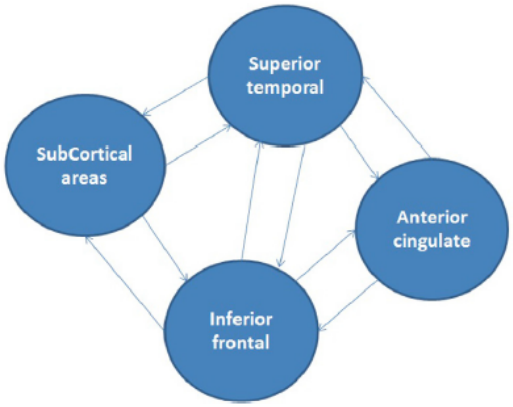

Fig. 3. The simplified anatomical model of interacting brain regions used for DCM estimation of effective connectivity parameters.

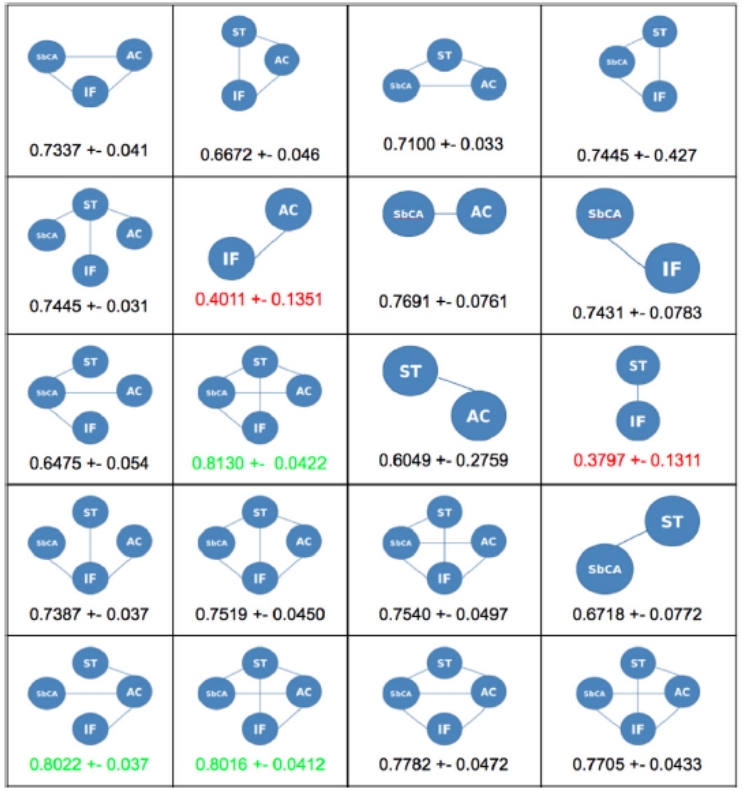

Fig. 4. The connections tested and their average and standard deviation of accuracy results in a classification by linear SVM on their coherence and delay values. Green values are above 80%. Red values are below random choice results. (For interpretation of the references to color in this figure legend, the reader is referred to the web version of this article.)

Ariadna Besga, Darya Chyzhyk, Itxaso Gonzalez Ortega, Jon Echeveste, Marina Grana-Lecuona, Manuel Grana, Ana González-Pinto White Matter Tract Integrity in Alzheimer's Disease versus Late Onset Bipolar Disorder and its Correlation with Systemic Inflammation and Oxidative Stress Biomarkers, Frontiers in Aging Neuroscience, 9:179
DOI https://doi.org/10.3389/fnagi.2017.00179

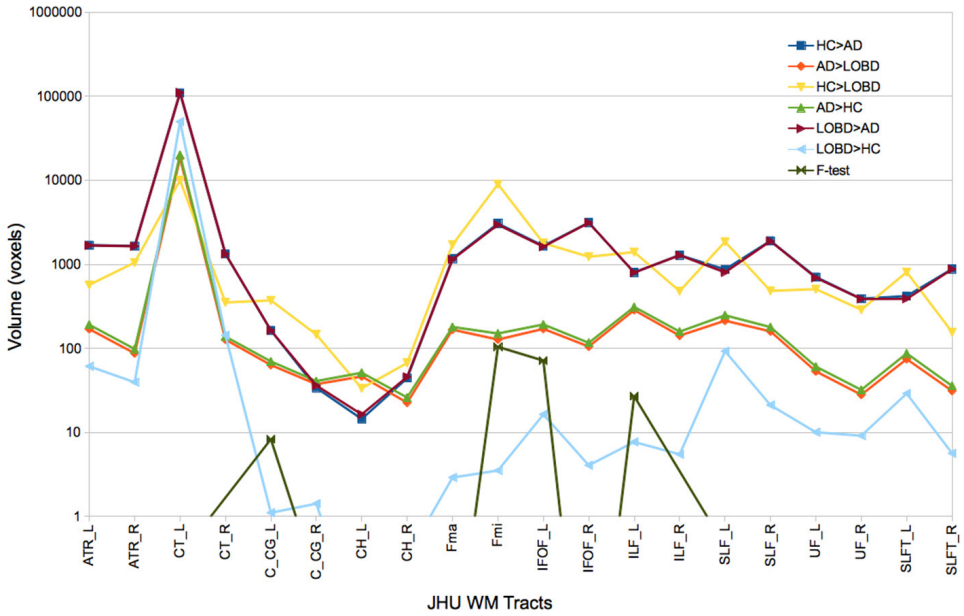

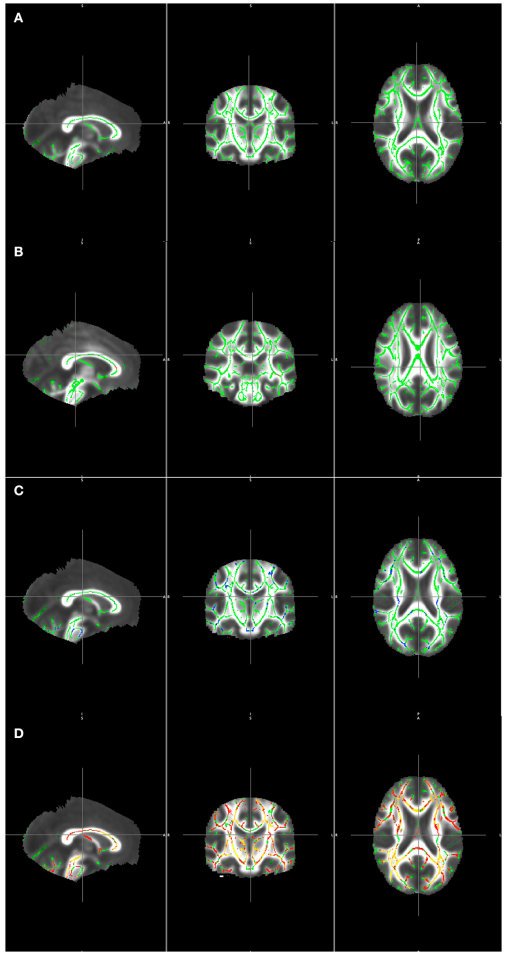

FIGURE 1 | Size of FA skeleton clusters found by each contrast (HC > AD, AD > LOBD, HC > LOBD, AD > HC, LOBD > AD,LOBD > HC, *F*-test) of the permutation test followed by TFCE cluster inference for each tract identified by the JHU White-Matter Tractography Atlas. R, Right; L, left; ATR, hemispheres of anterior thalamic radiation; CT, corticospinal tract; C_CG, cingulum (cingulate gyrus); CH, Cingulum (hippocampus); FMi, forceps minor; FMa, forceps major; IFOF, inferior fronto-occipital fasciculus; ILF, inferior longitudinal fasciculus; SFL, superior longitudinal fasciculus; UF, uncinate fasciculus; SLFT, temporal part of SLF .

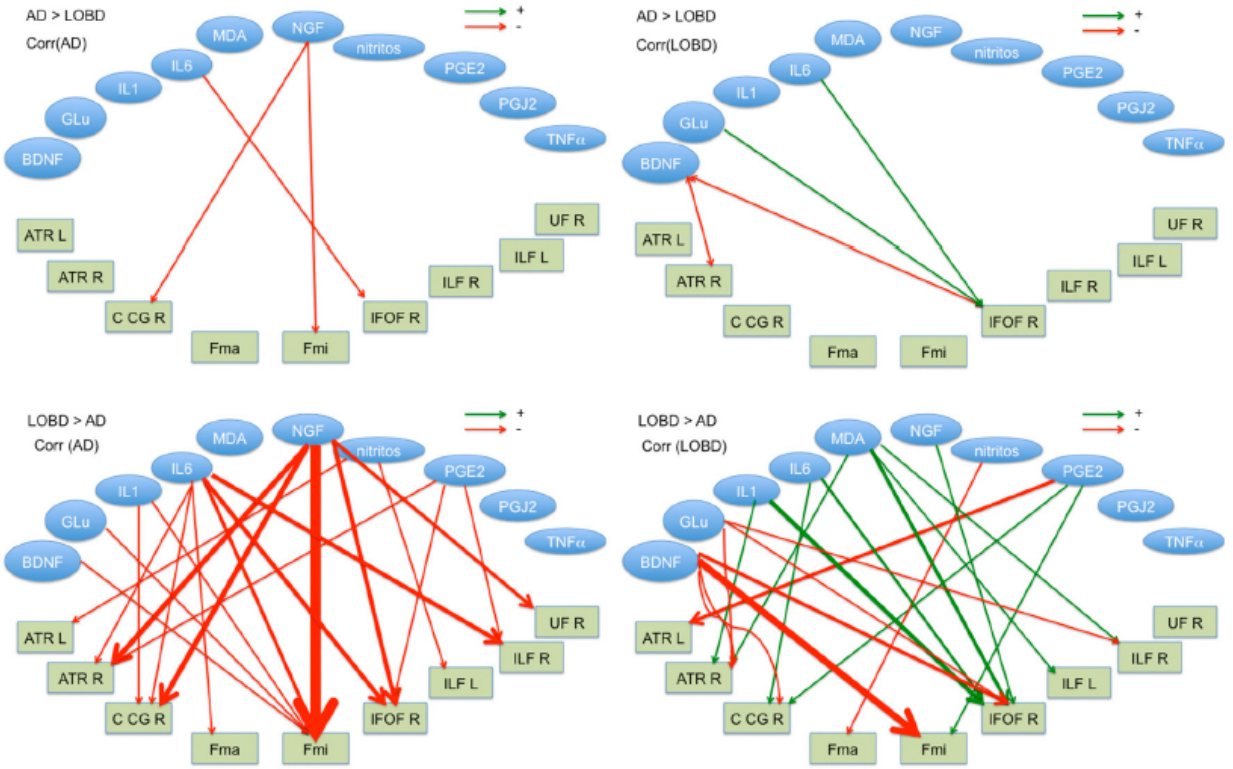

FIGURE 3 | Significant correlation ($p < 0.01$) between blood plasma biomarkers (ellipses up) and FA values at the TBSS clusters for AD > LOBD (up) and LOBD > AD contrasts, masked by the *F*-test, identified by the atlasquery tool (rectangles below). We report separate values for AD and LOBD populations (requested by reviewer). Red lines correspond to negative correlations, green lines correspond to positive correlations. Line width is proportional to the magnitude of correlation. R, Right; L, left; ATR, hemispheres of anterior thalamic radiation; C_CG, cingulum (cingulate gyrus); FMi, forceps minor; FMa, forceps major; IFOF, inferior fronto-occipital fasciculus; ILF, inferior longitudinal fasciculus; SFL, superior longitudinal fasciculus; and UF, uncinate fasciculus.

Behavior –motion- analysis

Motion analysis

- Human motion analysis
  - Entertainment
    - Games: human machine interface
    - Movies: image synthesis
  - Sports: performance analysis
  - Clinical: gait analysis, frailty, ASC diagnosisis
- Animal motion analysis
  - Phenotypical characterization
  - Analysis of animal models of human diseases
    - Alzheimer
    - Gender differences

Motion analysis

- Materials: imaging sensors are prominent
  - Signal processing
- Computational resources
  - Computer vision
  - Machine learning: activity modeling and recognition
    - A broad spectrum of techniques
    - Deep learning…..

Human motion capture systems

Inside In	Inside Out	Outside In
Electromechanical Suites	Electromagnetic	Marker-based Optical (active, passive markers)
Optical Fiber	Semi-passive	Marker-less Optical
Accelerometer Based	Optical	

Benefits

Portable	Could be portable	Not very portable
Can capture any motion anywhere	Low accuracy	Can be very precise

Human capture systems

- Electromechanical suite: exoskeleton/ armature worn over the subject
- Rods connected by potentiometers

Human motion capture systems

- Inertial sensors (gyros)
  - Accelerometer: measures acceleration
  - Gyroscope: measures orientation
  - Ultrasonic: measures distance

Pro:

- Real-time
- Inexpensive
- Self-contained
- No correspondences

Con:

- Restrictive
- No global position
- Can drift

[Xsens]

Optical human motion capture

- Subject surrounded by cameras
- Sensing is done at the cameras (and/or connected computers)
- Cameras need to be calibrated

Pro:

- Adaptable
- Minimally intrusive
- Highly accurate

Con:

- Limited in use (space need to be outfitted)

Optical (passive) Markers

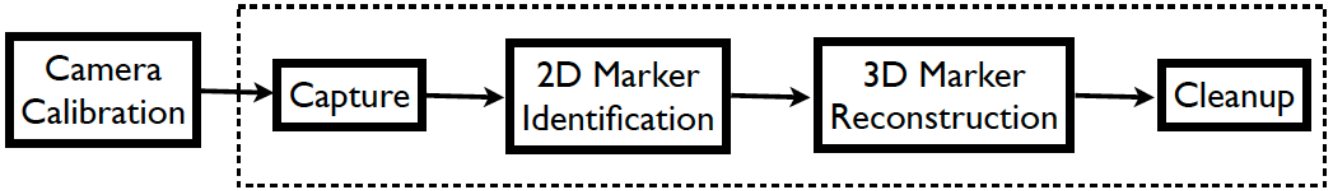

Typically:
40-50

Here:
300+

[Park & Hodgins, Siggraph 2006]

Reprepresentation: skeleton

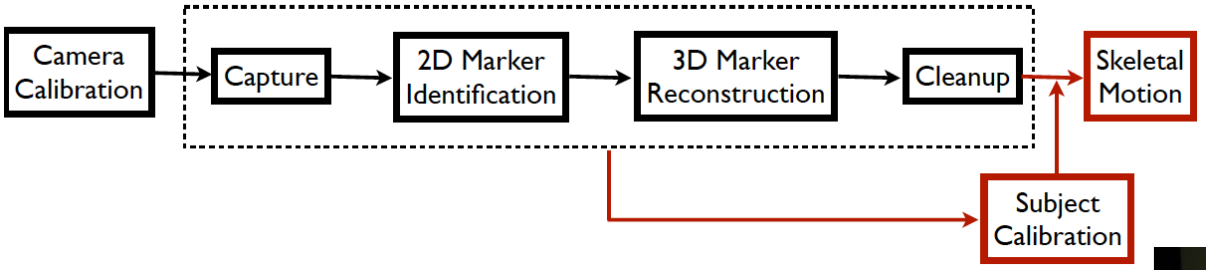

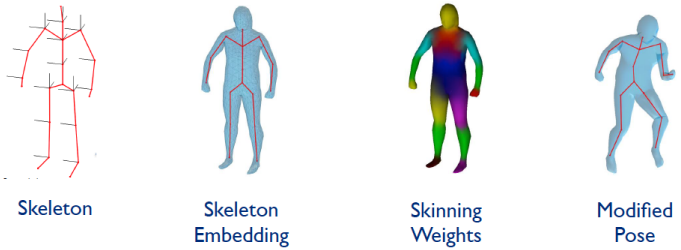

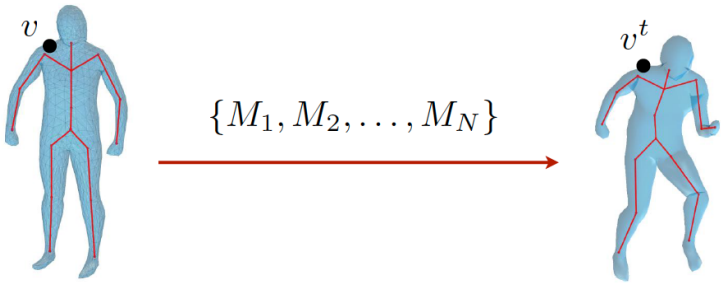

kinect

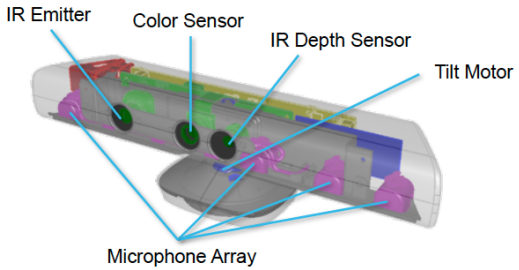

- Inexpensive and accurate depth camera / sensor
- 3D Pose estimation

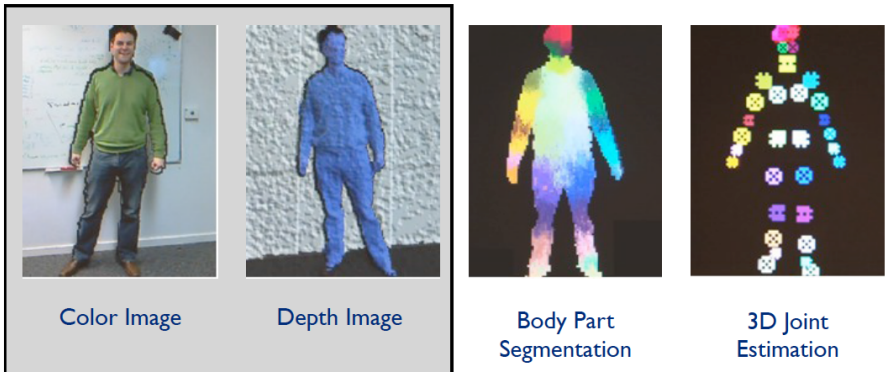

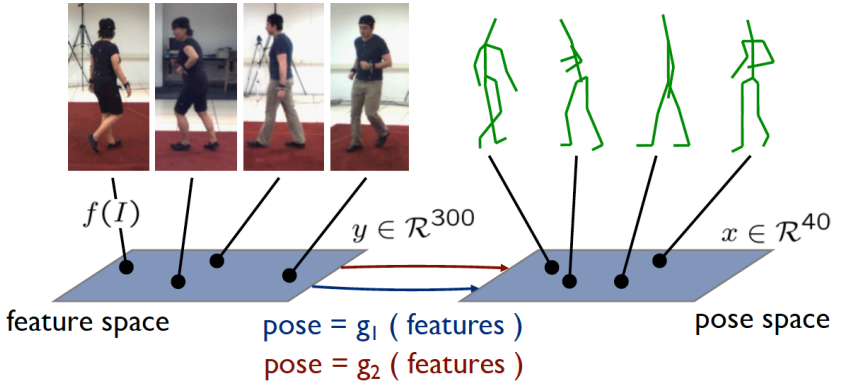

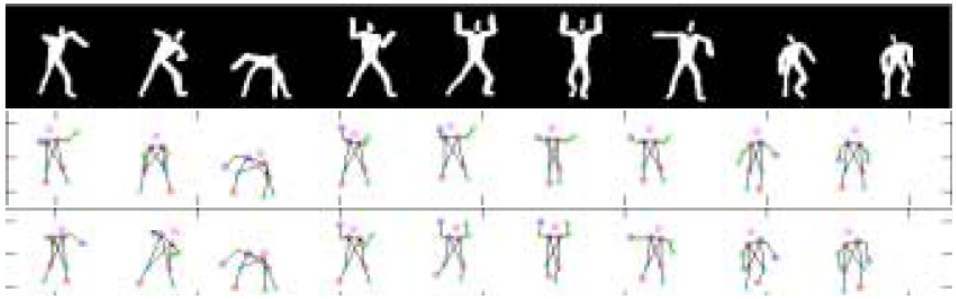

Realistic kinect detection

Multiperson pose estimation in video

Facial motion capture

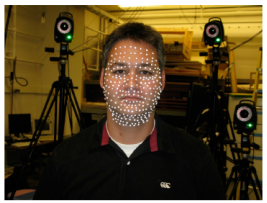

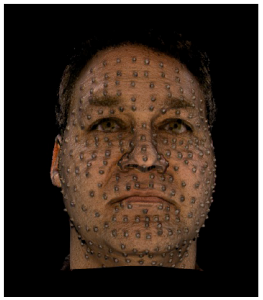

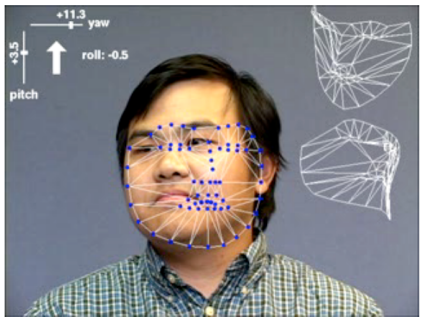

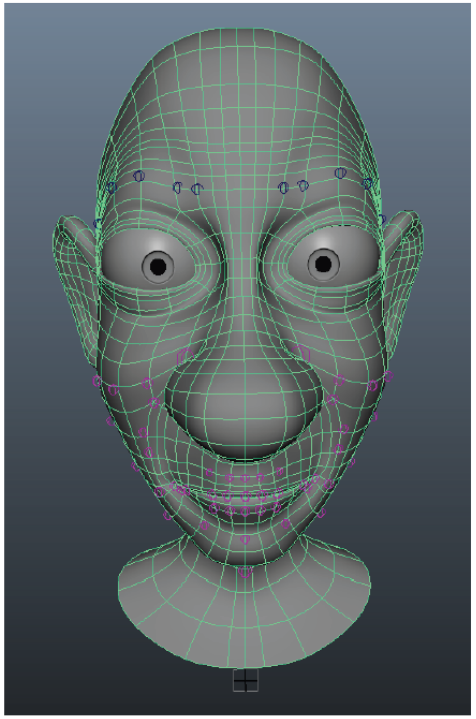

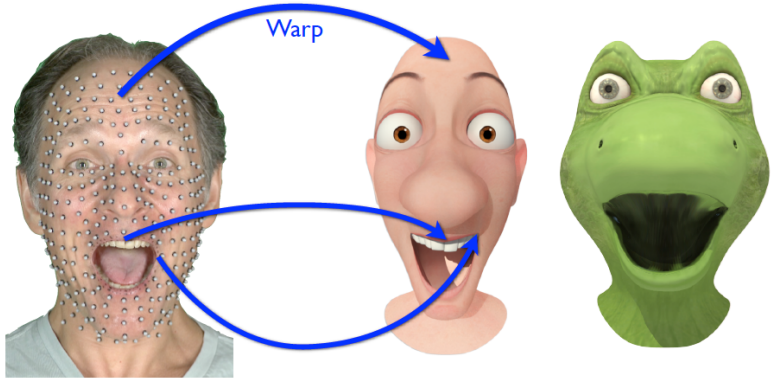

Human motion modeling

Autoregressive Models

First-order Markov Model

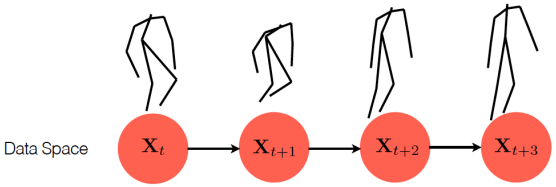

$$p(\mathbf{X}_t|\mathbf{X}_{t-1}) = \mathcal{N}(\mathbf{X}_t|\mathbf{D}\mathbf{X}_{t-1}, \Sigma)$$

Second-Order Markov Model

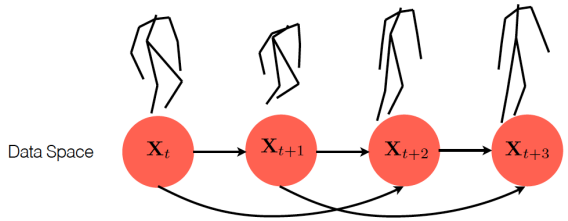

$$p(\mathbf{X}_1, \cdots, \mathbf{X}_F) = p(\mathbf{X}_1)p(\mathbf{X}_2|\mathbf{X}_1)\prod_{t=1}^{F} p(\mathbf{X}_t|\mathbf{X}_{t-1}, \mathbf{X}_{t-2})$$

Latent Variable Models

Linear Models

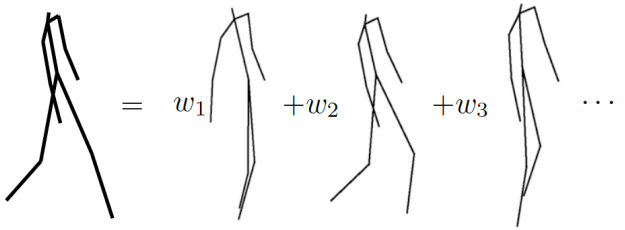

Graphical Model

Component Analysis

$$\mathbf{X}_t = \mathbf{B}\mathbf{Y}_t + \mu + \epsilon$$

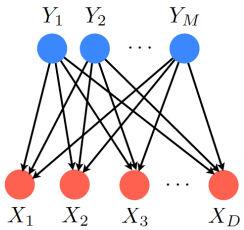

Automated home-cage behavioural phenotyping of mice
Hueihan Jhuang, Estibaliz Garrote, Xinlin Yu, Vinita Khilnani, Tomaso Poggio, Andrew D. Steele & Thomas Serre
NATURE COMMUNICATIONS | 1:68 | DOI: 10.1038/ncomms1064 |

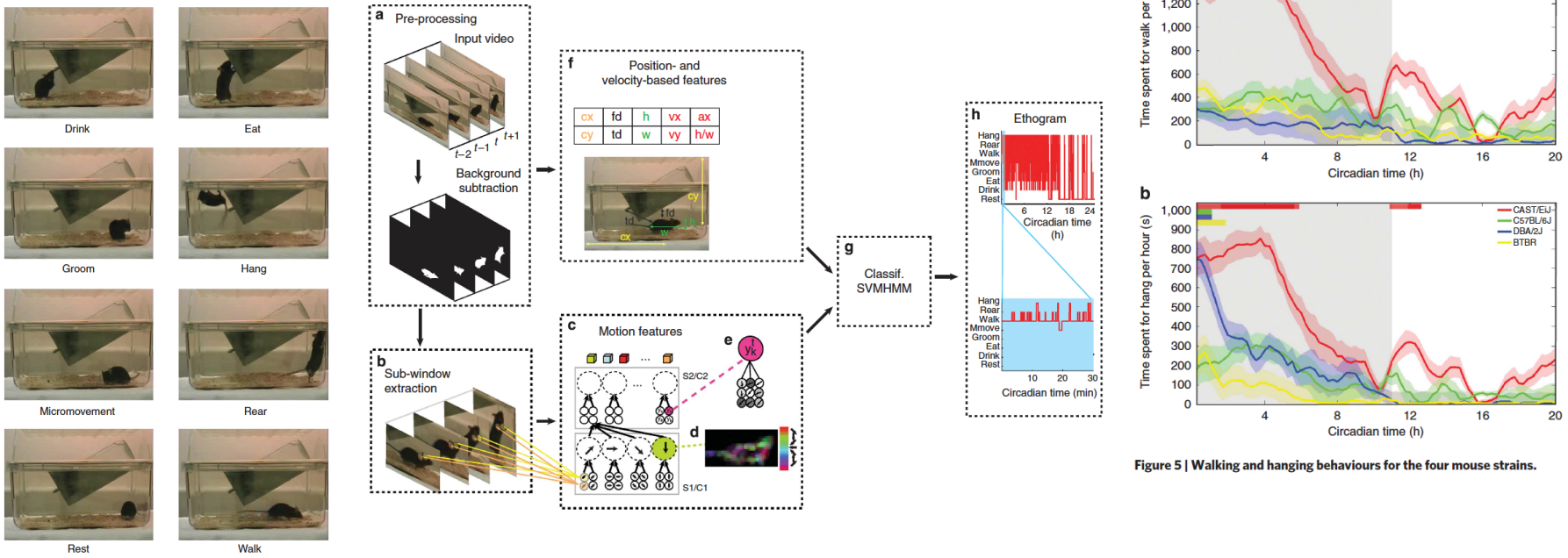

Figure 5 | Walking and hanging behaviours for the four mouse strains.

Facultad de informatica, Universidad Complutense de Madrid

28/02/2019

Pressure sensor

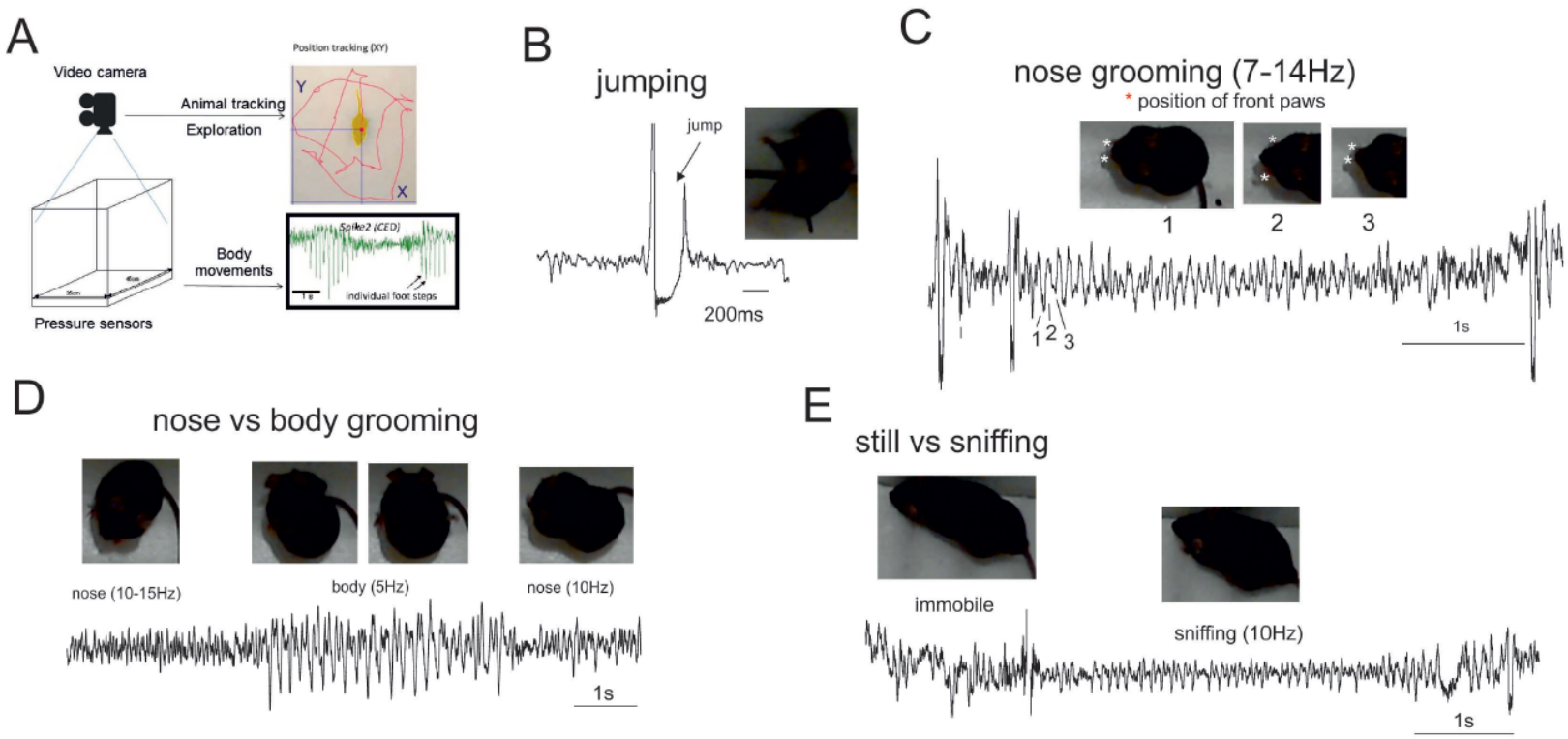

Xavier Leinekugel, The Neuroscience Institute in Bordeaux

Combined neural and behavioral analysis

Neuroethology

- Neural observation while recording behavior
  - MRI, EEG
  - Annotation, computer vision
- Neural intervention while recording behavior
  - Electrode implants (mice, rats)
  - Video recording
- Quantitative joint analysis of neural signal and behavior: scarce
- Behavior analysis: clustering (lack of labeled data)

Dean Mobbs, Jeansok J Kim,
Neuroethological studies of fear, anxiety, and risky decision-making in rodents and humans, Current Opinion in Behavioral Sciences,Volume 5,2015, Pages 8-15,https://doi.org/10.1016/j.cobeha.2015.06.005.

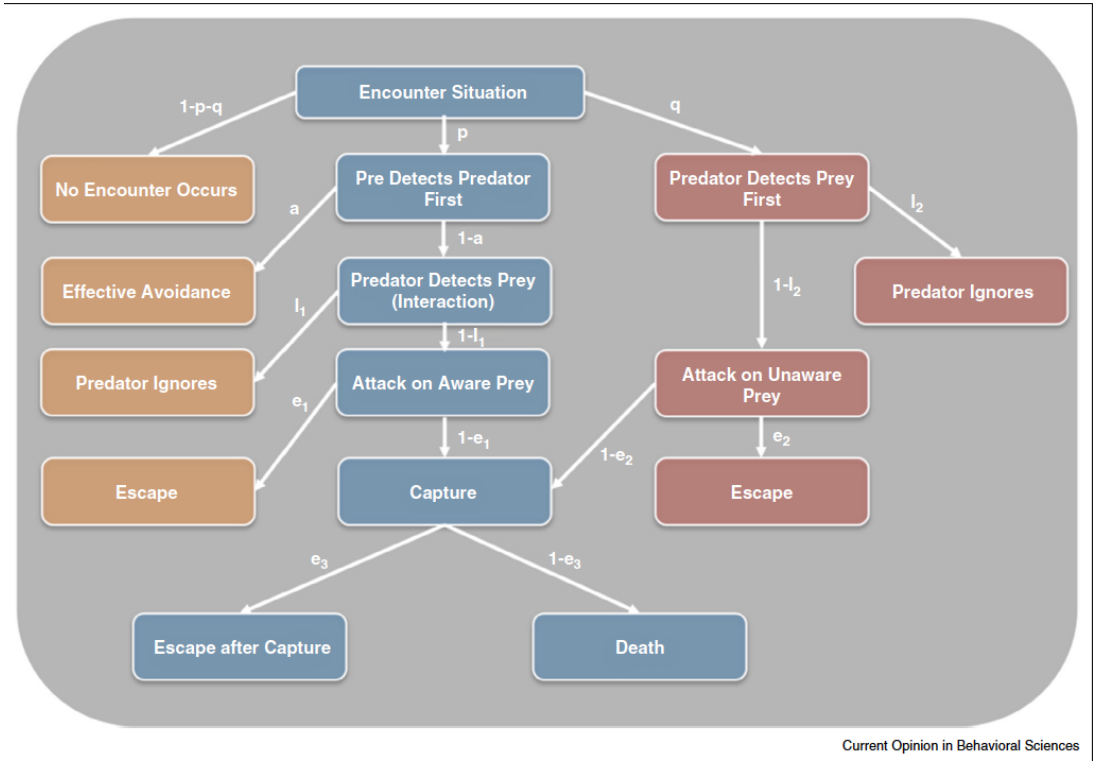

Current Opinion in Behavioral Sciences

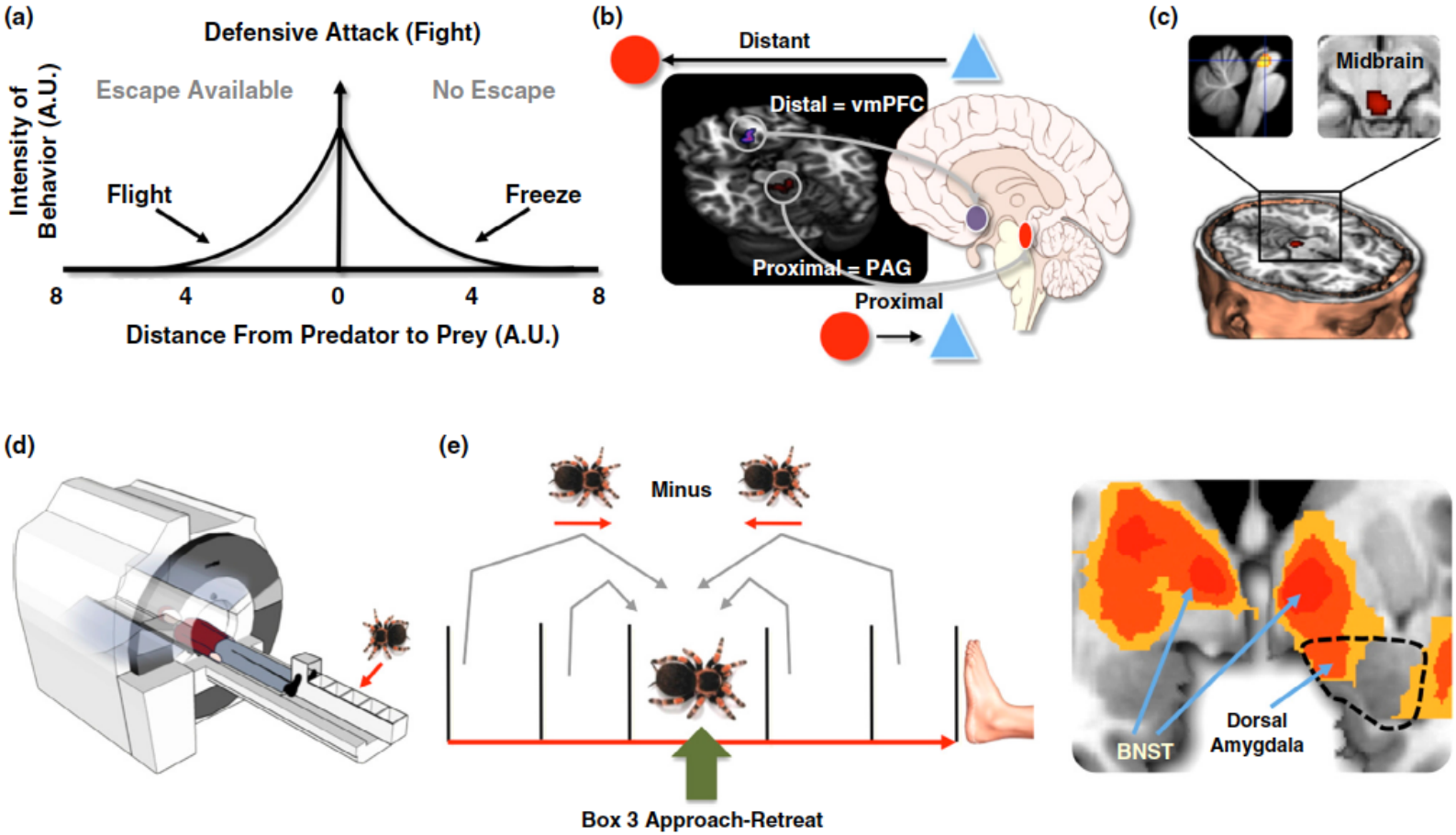

Current Opinion in Behavioral Sciences

(a) The Blanchard model proposing that physical distance to threat and escape (flight) availability evokes distinct defensive response. **(b)** The AET showing the neural switches between the vmPFC and PAG associated with distal and proximal threat and midbrain activity correlated with panic-related motor errors. **(c)** Experimental set up for oscillating tarantula task and **(d)** an example of monitoring the threats movement showing that as the Tarantula move closure based on it previous position compared to moving further away from a closure position there was increased activity in the dorsal amygdala and bilateral BNST.

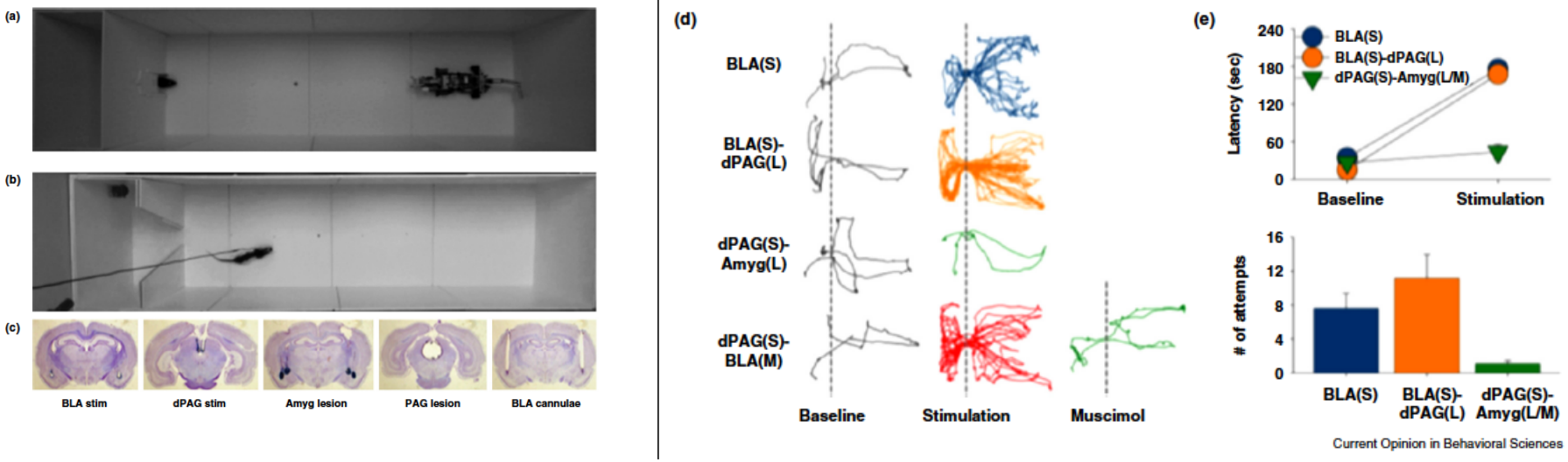

(a) A foraging rat facing a 'predatory' robot. Each time the rat approached the food pellet, the looming motion of the robot caused the rat to flee into the safety of the nest. Animals were unable to procure pellet located beyond certain distance but were able to retrieve pellet placed closed to the nest. **(b)** Same experimental design except either the amygdala or the dPAG is stimulated in naïve rats as they came near the pellet. Both amygdala and dPAG stimulation always elicited fleeing response in animals regardless of the pellet location. **(c)** Histology photographs show the tip locations for stimulation electrode and guide cannulae, and the extent of lesions. **(d)** Representative track plots from a rat with basolateral amygdala (BLA) stimulation, a PAG-lesioned rat with BLA stimulation, a BLA-lesioned rat with dPAG stimulation, and BLA-inactivated rat with dPAG stimulation. **(e)** Group mean (±SEM) latency to procure pellet (180 s = unsuccessful), and group mean (±SEM) number of times animals approached the pellet during the 180 s allotted time.

Discovery of Brainwide Neural-Behavioral Maps via Multiscale Unsupervised Structure Learning , Joshua T. Vogelstein,Youngser Park,Tomoko Ohyama, Rex A. Kerr, James W. Truman, Carey E. Priebe, Marta Zlatic.SCIENCE VOL 344 25 APRIL 2014

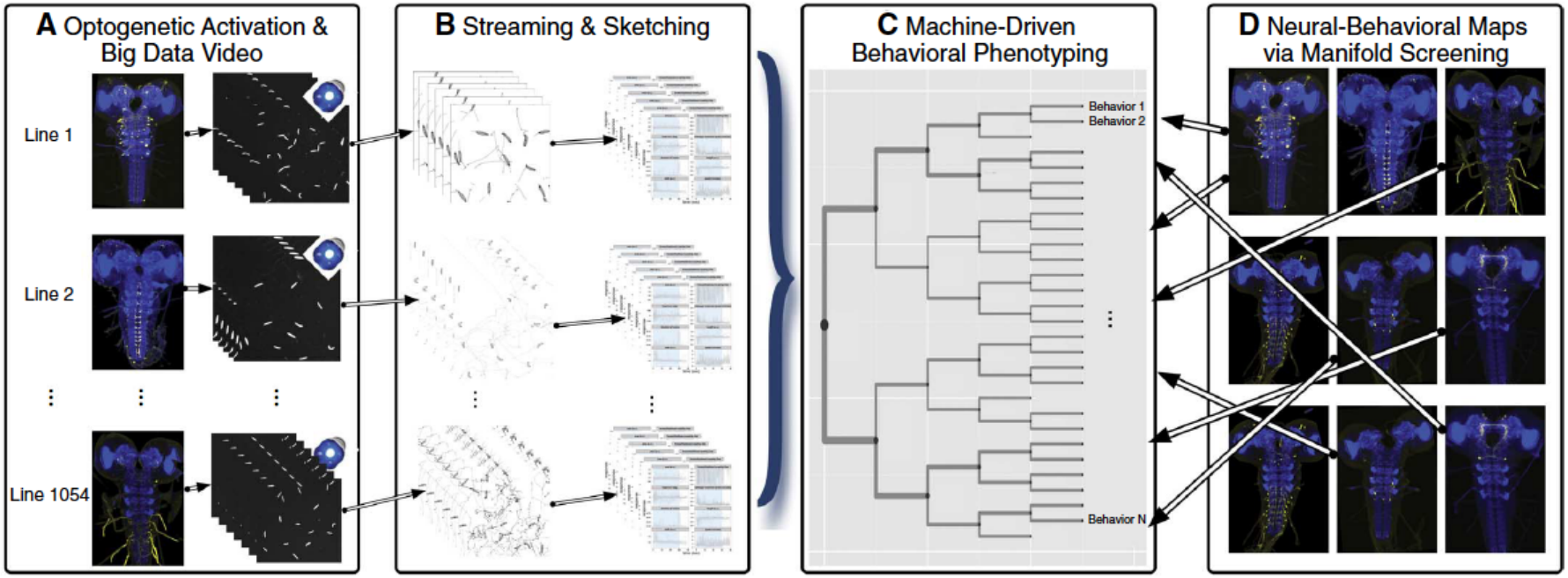

Fig. 1. Experimental design and methodology for obtaining neuron line–behavior maps. (**A**) Optogenetic activation screen of 1054 lines while digitally recording high-dimensional larval responses. (**B**) Streaming extracts the contours of each larva from each video frame; sketching extracts eight time-varying features from the contours that characterize the shape and motion of each animal. (**C**) Machine-driven behavioral phenotyping learns phenotype categories (called behaviotypes) from the sketches via multiscale unsupervised structure learning. (**D**) Manifold testing discovers which neuron lines evoke sets of behaviors that are different from negative controls, which facilitates associating each such line with some number of behaviotypes.

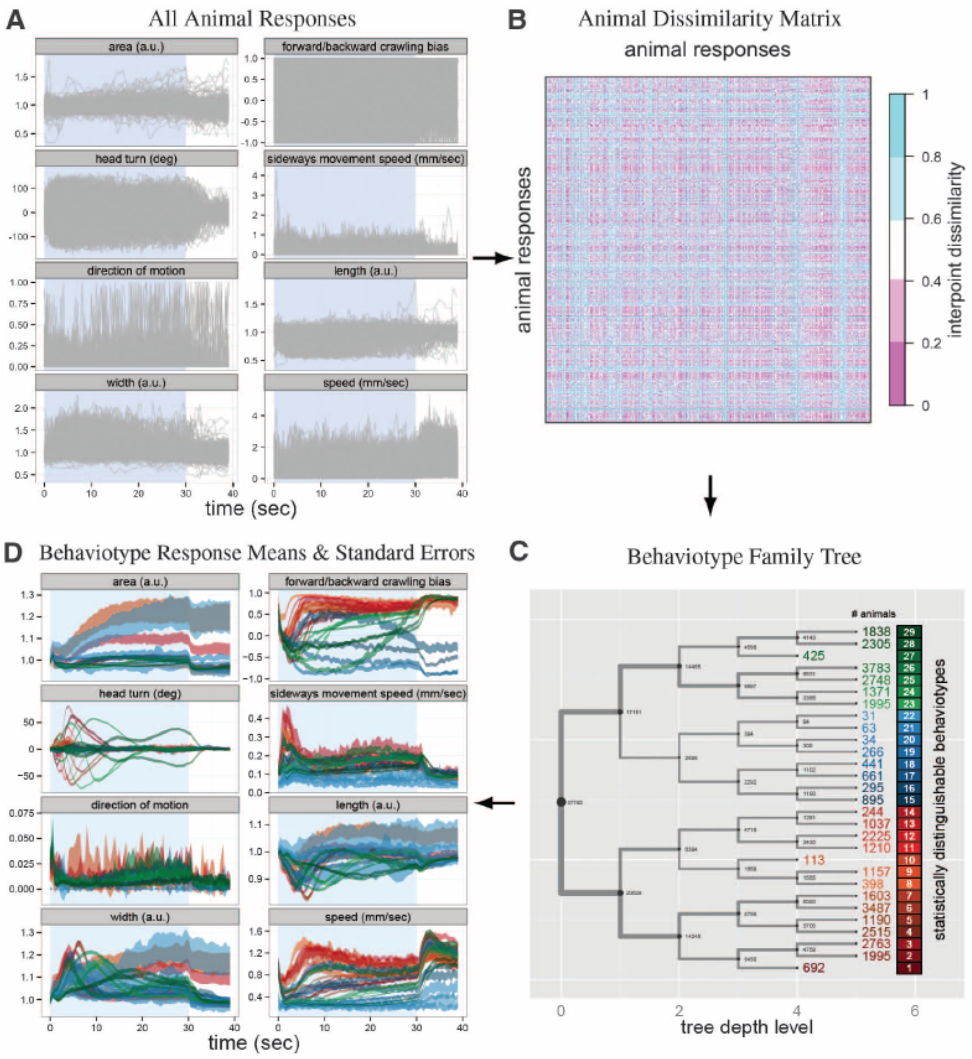
A
All Animal Responses
area (a.u.)
forward/backward crawling bias
head turn (deg)
sideways movement speed (mm/sec)
direction of motion
length (a.u.)
width (a.u.)
speed (mm/sec)
time (sec)
B
Animal Dissimilarity Matrix
animal responses
animal responses
interpoint dissimilarity
D
Behaviotype Response Means & Standard Errors
C
Behaviotype Family Tree
animals
statistically distinguishable behaviotypes
tree depth level

Toward a Science of Computational Ethology, David J Anderson and Pietro Perona, Neuron *84*, October 1, 2014

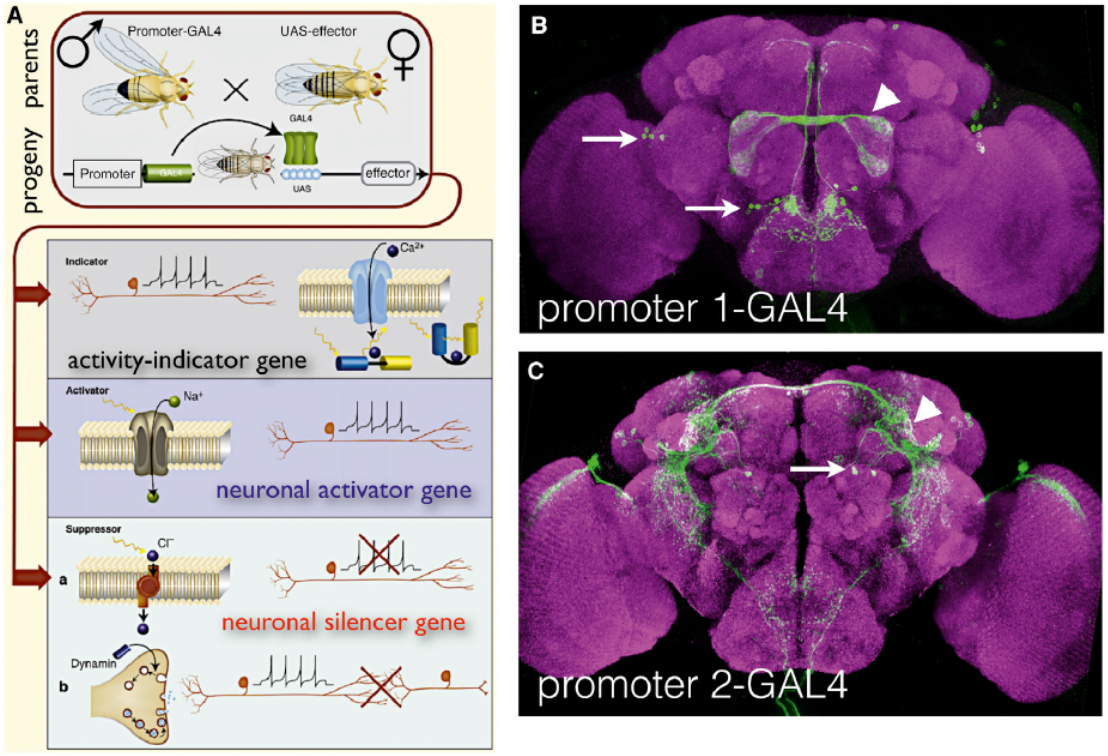

Figure 1. Mapping, Monitoring, and Manipulating Specific Neuron Populations in *Drosophila* Using the GAL4/UAS Binary System
(A) Upper: parental fly lines that contain a promoter-GAL4 or UAS-effector transgene (Table 1) are crossed to yield progeny that express GAL4, and therefore the UAS-effector, in a subpopulation of neurons defined by the specificity of the promoter (B and C). Lower: the effector can be an indicator to monitor the activity of the neurons, or ion channels or other genes to activate or silence the neurons. Reproduced with modifications by permission from Borst (2009).
(B and C) A fluorescent marker allows visualization of neurons identified by different promoter-GAL4 lines. Arrows indicate cell bodies (green dots); arrowheads indicate nerve fibers.

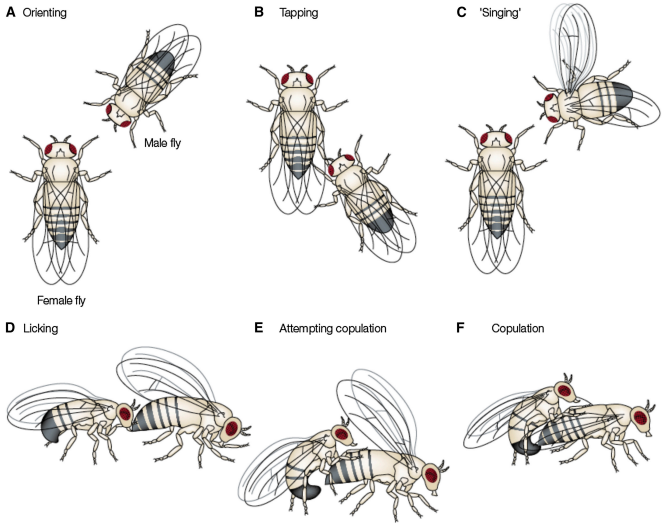
A Orienting
Male fly
B Tapping
C 'Singing'
Female fly
D Licking
E Attempting copulation
F Copulation

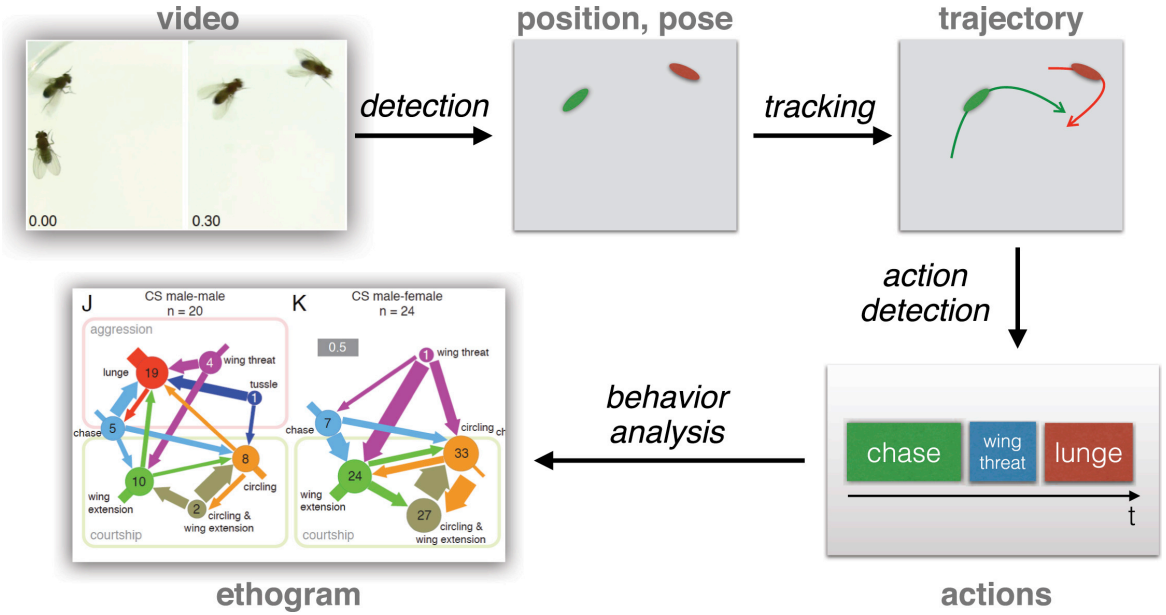
video
0.00
0.30
detection
position, pose
tracking
trajectory
action detection
chase
wing threat
lunge
t
actions
behavior analysis
J CS male-male n = 20
K CS male-female n = 24
aggression
courtship
ethogram

Increasing the throughput of behavioral analysis

Eight different behaviors (A) were automatically scored from video recordings of 20 flies walking in an arena. (B) Two minute trajectory of a single male fly detected among 20 in the arena. (C) Upper: raster plot for behaviors exhibited during the trajectory in (B); lower: translational and angular velocities superimposed on a 30 s segment of the raster plot. (D) Behavioral "vectors" for female, male, and fru1/fru1 mutant male flies. Each column represents a single fly and each row a single behavior. Numbers at top refer to experiment and number of flies tracked.

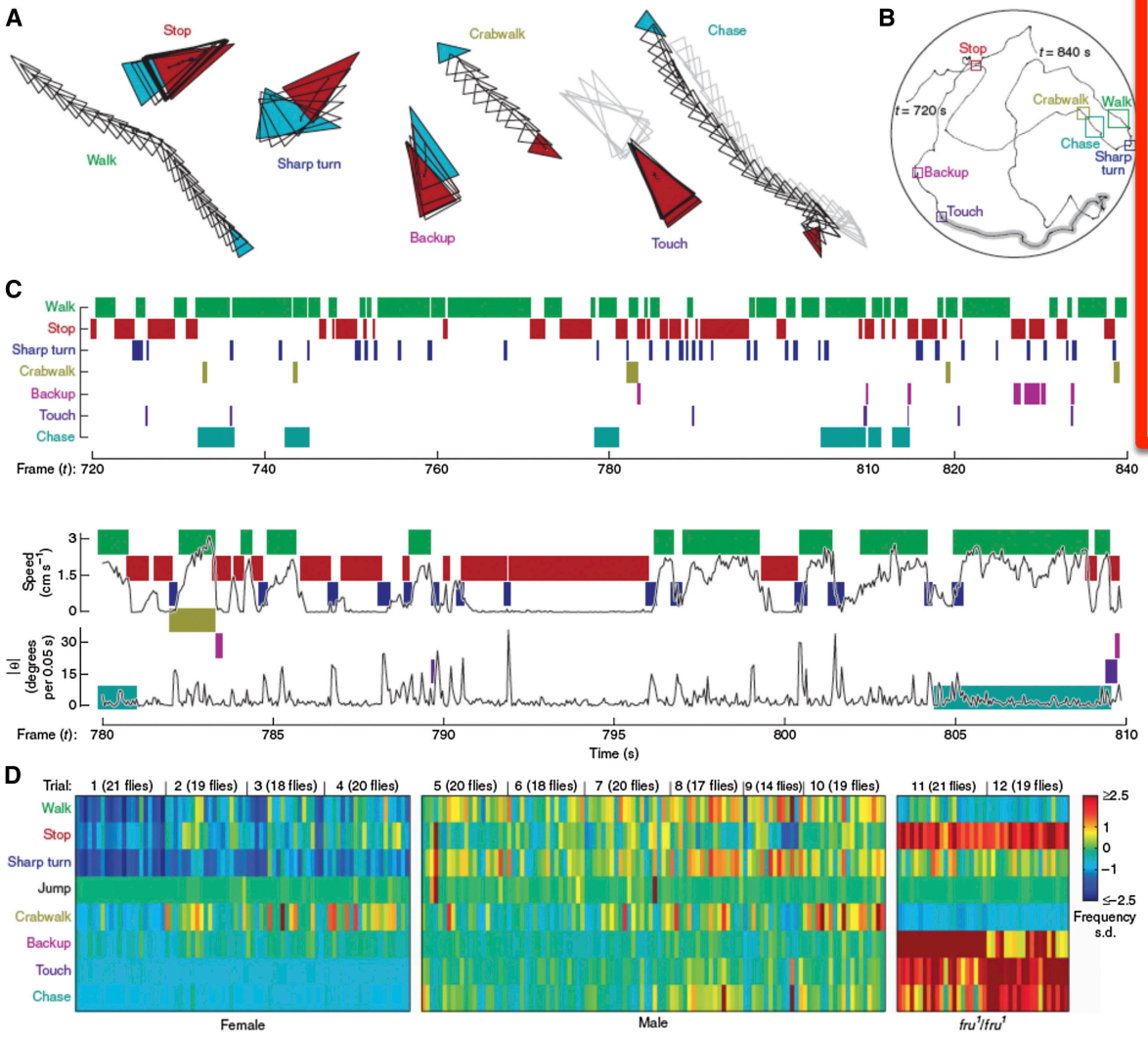

tracking systems to measure the individual trajectories of dozens of flies simultaneously in an arena

Neuron 2014 84, 18-31DOI: (10.1016/j.neuron.2014.09.005

The case study of CybSPEED

CybSPEED proposal

- **Cyber-Physical Systems for PEdagogical Rehabilitation in Special Education**
- Aim : to advance a novel framework for
  - analysis, modelling, synthesis and implementation
  - of Cyber-Physical Systems
  - for pedagogical rehabilitation in special education,
- based on a combination of
  - brain-aware robotics, cognitive biometrics, computational intelligence and reasoning in
  - humanoid and non-humanoid robots for education.

CybSPEED proposal

- CybSPEED project emphasizes the intrinsic-motivational approach to learning
  - by designing human-robot situations
    - (games, pedagogical cases, artistic performances)
  - And advanced interfaces
    - (brain-computer, eye-gaze tracking and virtual reality)
- Where students interact with the novel technology
  - to enhance the underlying self-compensation and complementarity of brain encoding during learning.

CybSPEED proposal

- Technical Research on three levels
  - Analysis of cognitive biometrics signals,
  -
  - Modeling the learner-robot interaction and
  - Development of novel instruments
    - towards an optimal design of Cyber-Physical Systems
    - for improved pedagogical rehabilitation in education

Consortium and partners

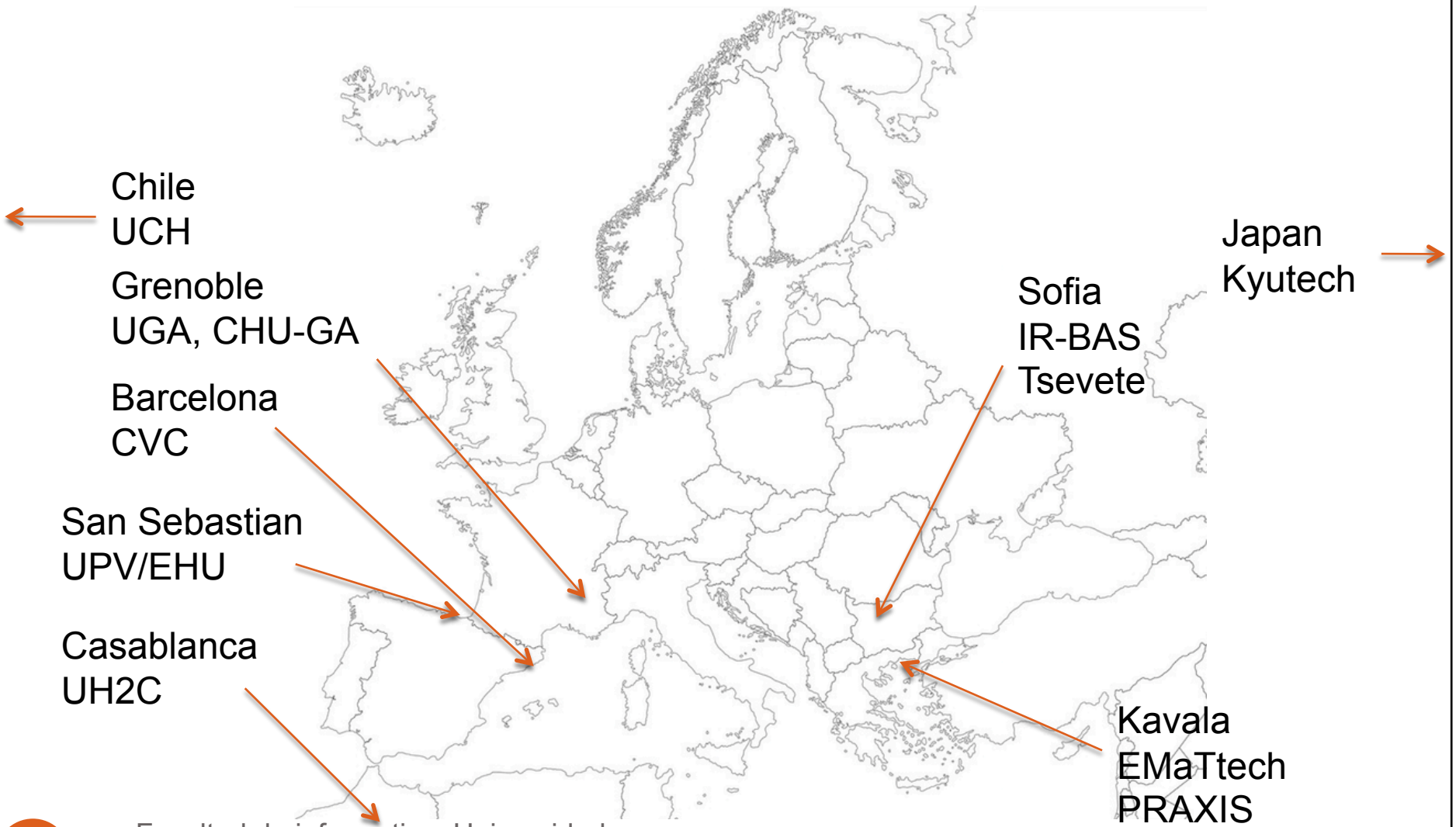

Knowledge topology of the project

Artificial perception

User awareness

CVC

UCH

Robot soft-adaptation

IR-BAS

Advanced human-robot interfaces

UPV/EHU

Games and storytelling

Tsevete

Student progression measurement

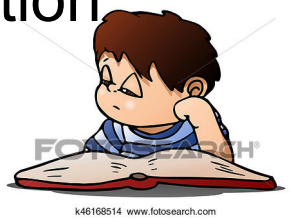

Kyutech

Behavior measurement

UGA

CHU

PRAXIS

EMaTTech

UH2C

Neural activity correlation with behavior

- Some experiment is focused on children with autism spectrum disorders (ASD)
- Recruited from the population of children under treatment in some care center,
- The experiment is designed as a longitudinal experiment, where the same children will be exposed to the robot in several sessions along a period of one year.
- The main hypothesis of the experiment is that the presence of the anthropomorphic robot has a definitive effect on the attention of children with ASD.

Research questions

- Is there any gender difference in response to the Nao robot in children with ASD?
- Is there an effective difference in response to the human teacher versus the Nao in children with ASD?
- Are there differences in response to Nao among diverse special kinds of ASD?
- Is there any time effect on the long term exposure of the children to Nao?

An experimental setting for neuroethological human robot interaction?

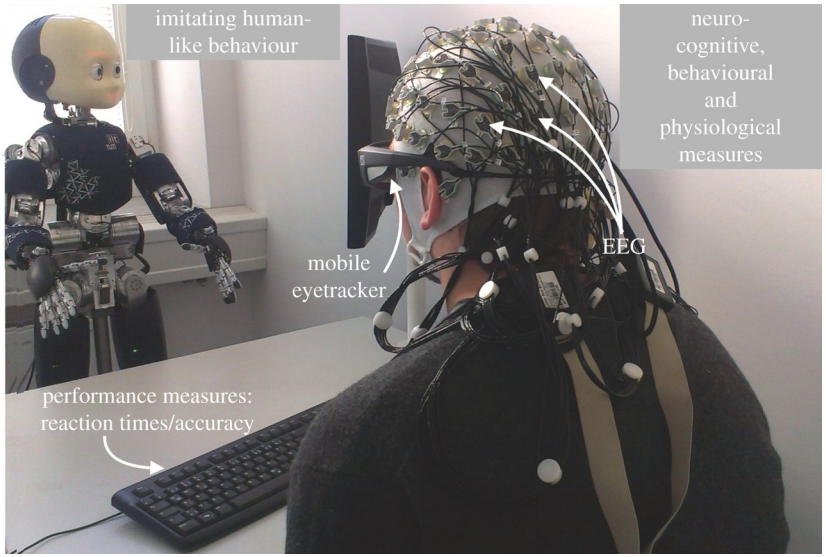

Too far from **ecological validity** in special educational needs!

A more appropriate setting

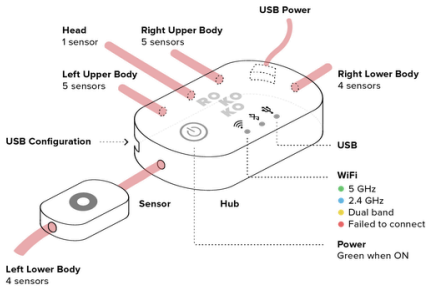

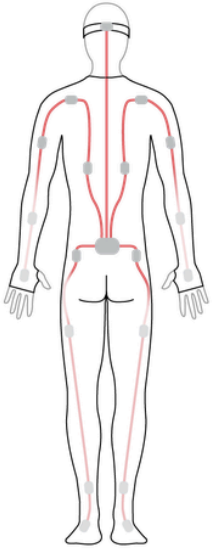

An approximation to the desirable setting

Conclusions

Conclusions

- There are several animal models that are working
  - Wide opportunities to apply machine learning techniques
  - Incresing social pressure against animal experiments (ethics constraints)
- Human applications face the ecological validity problem
  - Increasing ethics and data protection constraints for experimentation

Conclusions

- Computational ethology is a wide avenue for signal processing and artificial intelligence applications and developments
- Computational neuroethology is the next big step in the understanding of the brain
- Requires close connection with people from medicine, neuroscience, biology,…
  - Computer science at the service of…
  - Ethics and personal data protection …

ACKNOWLEGEMENTS

Slide materials borrowed from Yasher Sheikh CMU course on Human Motion Modeling and Analysis 2012